

On the influence of peatland draining on local climate

Ari Venäläinen, Laura Rontu and Reijo Solantie

Finnish Meteorological Institute, P.O. Box 503, FIN-00101 Helsinki, Finland

Venäläinen, A., Rontu, L. & Solantie, R. 1999. On the influence of peatland draining on local climate. *Boreal Env. Res.* 4: 89–100. ISSN 1239-6095

In no other country has the draining of peatland taken place to such a large extent as in Finland. According to earlier studies based on an analysis of observed temperatures, this draining has lowered the night-time minimum temperatures in heavily-drained regions. In the present study, we simulated the cooling effect using the HIRLAM numerical weather prediction model. When simulated wet and dry peat conditions were compared in a late summer clear and calm case leading to night frost, the drop in local night-time minimum temperatures reached ten degrees. The difference in temperature was caused mainly by the change in the soil heat flux.

Introduction

Human activities have modified the environment in many ways having an influence on the climate and weather. Model simulations of the influence of the large-scale deforestation of the Amazon Basin are perhaps the best-known studies relating to the human influence on the atmosphere by changing the earth surface properties (e.g., Shukla *et al.* 1990). According to these studies, large-scale deforestation would change the surface energy balance, increase the temperature and decrease precipitation. Due to the decrease of precipitation the conditions would become unfavourable for re-establishing the forest. In the boreal zone the influence of changes in the environment has been studied e.g. by Bonan *et al.* (1992). According to their research, changes in boreal zone vegetation, such as the replacement of forests with tundra, may initiate feedbacks, which could also extend to lower latitudes. These results are based

on simulations made with a global climate model.

A man-made environmental change that may have had an influence on climate in some regions in Finland is, according to Solantie (1994), the wide-scale draining of peatlands. Peatlands were drained in order to create favourable conditions for the growth of new forest. Draining has been very intensive, especially in the middle boreal zone of Finland, located between 62°N and 67°N. In some parts of this zone the fraction of drained area exceeds 50% of the total area; on average the fraction is 30% (Finnish Forest Research Institute 1992). Most of the draining activity occurred between 1960 and 1980. There are now forests in places where open bogs used to be the prevailing terrain type some 30 years ago, with the exception of those areas where draining was not successful. In no other country has the draining of peatlands taken place to such a large extent as in Finland and therefore this influence may be peculiar to this country.

The possible temporary climatic consequences of peatland draining are connected with the changing properties of the soil and surface. During clear summer nights the radiative cooling of the surface is to a large extent balanced by the soil heat flux and this soil heat flux changes when the soil moisture changes. Drained, dry peat is a very effective heat insulator, almost totally preventing heat flow from deep soil layers to the atmosphere. Long-wave radiation cools open peatlands effectively and if there is no compensating heat flow from the soil, the minimum temperatures drop.

The magnitude of the temperature drop was estimated by Pessi (1957), Latja and Kurimo (1988) and Solantie (1994), who compared temperature measurements in different peat areas. According to their results, the drainage of peatlands cooled surface temperatures from 0.1 °C to 1.4 °C, depending on month, height of the temperature measurement and proportion of drained peatlands in the area. According to Solantie (1994) the nocturnal cooling phenomenon continues for about 15 years after the drainage, that is, until afforestation begins to influence the surface long-wave radiation balance via the appearance of canopy shelter.

Soil drainage also has a minor influence on the radiative properties of the surface. The long-wave emissivity of the surface is smaller for a dry than for a wet surface. The decrease of the outgoing long-wave radiation due to the emissivity change thus counteracts the cooling effect caused by the decrease of the heat flux from ground. The surface albedo (the ratio of reflected shortwave radiation to incoming shortwave radiation) of peatlands is on average greater than that of forest. In the longer term, the decrease of albedo leads to increased absorption of short-wave radiation and further to an increase in daily maximum temperatures (Solantie 1994).

The surface roughness of forest is greater than that of peatland. When forests become fully grown, the latent heat flux increases due to enhanced mixing and transpiration (Solantie and Ekholm 1988), leading in turn to a decrease in daytime temperatures.

In the current study the former empirical results are compared with model simulations. The simulations were made using a one-dimensional

version of the HIRLAM numerical weather prediction model. The aim of the model simulations was to reveal the possible effect of changing soil and surface properties on the surface energy balance and on the predicted near-surface temperatures.

Methods

The HIRLAM numerical weather prediction model

A one-dimensional version of the HIRLAM short-range numerical weather prediction model was used to study the influence of changing soil properties on the predicted near-surface temperatures. The HIRLAM model is developed by and used for operational weather prediction in nine European national weather services. The one-dimensional model version is used for research. It includes all the physical parametrization schemes of the model including soil processes, soil-atmosphere interaction, clouds and condensation, turbulence in the atmospheric boundary layer and radiation. The calculations are made for a soil-atmosphere column starting at a depth of about one metre below the surface and reaching a height of about 30 km in the atmosphere.

The HIRLAM soil scheme used in our experiments is described in Källen (1996) and Savijärvi (1992). We give a brief overview here. The scheme describes the evolution of soil temperature and water content by solving simple prognostic equations. The influence of snow and ice is also included into the scheme for winter conditions.

In a thin layer of soil with heat capacity c_s (J kg⁻¹ K⁻¹), density r_s (kg m⁻³) and thermal conductivity l_s (W m⁻¹ K⁻¹) the temperature change is due

to the convergence of vertical heat flux $G = -\lambda_s \frac{\partial T}{\partial z}$ in the layer,

$$\frac{\partial T}{\partial t} = \frac{1}{\rho_s c_s} \frac{\partial G}{\partial z}. \quad (1)$$

If c_s , ρ_s and λ_s are constants and z (m) is the vertical coordinate, the basic diffusion equation can be written as

$$\frac{\partial T}{\partial t} = -\kappa \left(\frac{\partial^2 T}{\partial z^2} \right), \quad (2)$$

where $\kappa = \frac{\lambda}{c_s \rho_s}$ ($\text{m}^2 \text{s}^{-1}$) is the soil diffusivity, T (K) is the temperature and t (s) is time.

The temperature can be solved from Eq. 2 when the boundary values are given. Deep in the soil at $z = z_B$ the temperature is assumed to have a climatological value, T_c , constant during the model integration,

$$T(z_B) = T_c. \quad (3)$$

At the surface ($z = 0$), the energy flux is continuous, i.e., the sum of the atmospheric energy fluxes F equals the net soil heat flux,

$$F(0) = G(0), \quad (4)$$

where $F(0)$ is given by the surface energy balance equation,

$$F(0) = \text{SW}(0) + \text{LW}(0) + H(0) + \text{LE}(0). \quad (5)$$

Here SW is the net short-wave and LW the net long-wave radiation flux, H is the sensible and LE the latent heat flux (all given in W m^{-2}).

The sensible and latent heat fluxes at the surface are calculated from diagnostic formulae using information about the temperature, humidity and wind at the lowest atmospheric model level and about the surface, represented by the temperature of the uppermost soil layer and surface wetness. We calculated the fluxes according to the Monin-Obukhov similarity theory, which takes into account surface roughness and the stability of the surface layer. Vertical diffusion in the atmospheric boundary layer above the surface layer is calculated using the approach proposed by Louis (1979). The net radiative fluxes are calculated according to the HIRLAM radiation scheme based on Savijärvi (1990). The radiation scheme parameterizes the influence of the main atmospheric gases, aerosol and clouds on radiation at all model levels and at the surface. Cloud water amount and cloud cover are provided by the model's condensation scheme based on Sundqvist *et al.* (1989) and Sundqvist (1993). The surface long-wave emissivity and short-wave albedo are used as input for the radiation scheme.

The HIRLAM model uses a three-layer soil

scheme. For temperature, Eq. 2 and the boundary conditions Eqs. 3–5 now lead to

$$\frac{\partial T_s}{\partial t} = \frac{F}{\rho_s c_s D_1} + \frac{\kappa(T_d - T_s)}{0.5D_1(D_1 + D_2)}, \quad (6)$$

$$\frac{\partial T_d}{\partial t} = -\frac{\kappa(T_d - T_s)}{0.5D_2(D_1 + D_2)} + \frac{\kappa(T_c - T_d)}{0.5D_2(D_2 + D_3)}, \quad (7)$$

where T_s and T_d are the temperatures of the uppermost and the middle layer with thickness of $D_1 = 7$ cm and $D_2 = 42$ cm, respectively. $D_3 = 42$ cm is the distance between the centres of the second and the third soil layers.

Eqs. 6 and 7 are solved by an implicit time-stepping procedure. A time filter is used to connect the odd time steps with the even ones.

The screen-level temperature T_{2m} and dew-point temperature T_{d2m} are calculated diagnostically using the temperature and humidity values at the lowest atmospheric model level together with the temperature and soil water content in the uppermost soil layer.

The soil water content is calculated from diffusion equations analogous to Eqs. 2, 6 and 7 including the soil hydraulic diffusivity parameter instead of the soil thermal diffusivity. The surface forcing is obtained as the sum of evaporation and precipitation. The precipitation flux is calculated by the condensation scheme. We used the climatological value of soil water content deep in the soil, which was kept constant during the integration.

Model experiments

The aim of the numerical simulation experiments was to reveal the importance of the changing soil and surface properties for the predicted near-surface temperatures. In the simulations we varied the parameters influencing Eqs. 5–7, i.e., the soil density, heat capacity and thermal conductivity, as well as the surface albedo, emissivity and roughness length. We chose typical values for open natural wet peatland, open dried peatland without forest and with some forest already growing (Table 1). The same values for the soil properties were used in all soil layers of the model. The albedo values were based on the results of Solantie (1988). The values of the soil properties

for dry and saturated peat, surface emissivity and roughness length were taken from Oke (1987).

To create a realistic environment for the model experiments, a representative region and season were chosen and the dynamical tendencies of atmospheric variables from full three-dimensional HIRLAM runs were included. The experiments were made for Kauhava (63°06'N, 23°02'E), situated in western Finland in a region where large peatland areas have been drained. The simulations were run for 24 hours starting at 12 UTC 14 August, 00 UTC and 12 UTC 15 August, 1997. During the selected period the nights were cool and clear and the first night frost at Kauhava during summer 1997 occurred on 16 August.

Initial values for soil temperature and water content were defined according to Table 2. The deep soil temperature T_c represents a climatological mean value (Heikinheimo and Fougstedt 1992). The volumetric moisture content of peat may exceed 50%. In the experiment a maximum value of 29% was used to represent wet soil in the moisture calculations, because it is the maximum soil water content allowed in HIRLAM in order to guarantee the numeric stability of the model. Note that the soil moisture so defined does not influence the soil thermal properties but solely the hydrologic cycle of the

model.

The number of vertical levels in the one-dimensional experiment was 61. The lowest model level is at a height of about four metres above the surface. A time-step of two minutes was used. Initial values and the large-scale dynamical tendencies of temperature, humidity, wind and surface pressure for the one-dimensional experiment were provided by the corresponding three-dimensional HIRLAM experiments at the grid point nearest to Kauhava.

We compared the values predicted by the model for screen level temperature T_{2m} and surface temperature with the values available from synoptic observations. Exact correspondence with observations was not expected, as the initial state of the simulations was not fully defined by the observations.

Net-radiation values obtained from the model simulation were also compared with values that were calculated with the help of synoptic observations. The global radiation parameterization used is explained in detail in Venäläinen and Heikinheimo (1997) and Iqbal (1983). The long-wave radiation balance was calculated using a formula obtained from Brutsaert (1982). A short description of the parameterizations is given in the Appendix.

Table 1. Typical values used in the experiments for the soil density ρ_s (kg m^{-3}), specific heat c_s ($\text{kJ kg}^{-1} \text{K}^{-1}$), thermal conductivity λ_s ($\text{W m}^{-1} \text{K}^{-1}$), surface albedo α (%), surface emissivity ε (%) and roughness length z_0 (m). The values are valid for all three soil layers in the model.

Simulation	ρ_s	c_s	λ_s	α	ε	z_0
Wet surface, no trees	1 100	3.65	0.482	14.5	99	0.1
Dry surface, no trees	300	1.92	0.058	14.5	95	0.1
Dry surface, forest	300	1.92	0.058	11.5	95	0.5

Table 2. Initial values of the soil temperature (T , °C) and soil volumetric water content (W , %) in the three soil layers (s = surface, d = middle and c = deep) of the model.

Simulation	T_s	T_d	T_c	W_s	W_d	W_c
14 Aug 12 UTC wet soil	14.5*	13.8*	12.0	24.3	25.7	28.6
14 Aug 12 UTC dry soil	14.5*	13.8*	12.0	14.3	14.3	21.4
15 Aug 00 UTC wet soil	8.2*	13.3*	12.0	24.3	25.7	28.6
15 Aug 00 UTC dry soil	8.2*	13.3*	12.0	14.3	14.3	21.4
15 Aug 12 UTC wet soil	16.2*	13.6*	12.0	24.3	25.7	28.6
15 Aug 12 UTC dry soil	16.2*	13.6*	12.0	14.3	14.3	21.4

*Initial values from a three-dimensional HIRLAM simulation

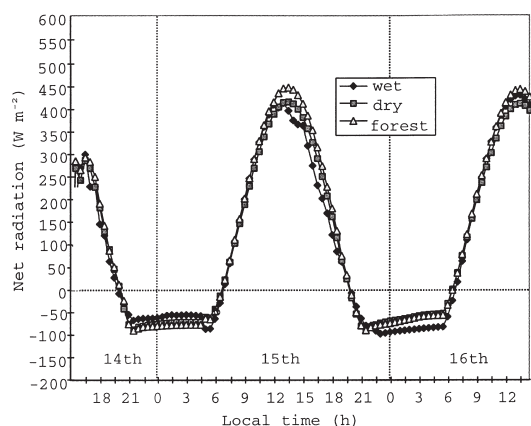


Fig. 1. Simulated radiation balance for the Kauhava weather station location, 14–16 August 1997. Downward fluxes are positive.

Results

In the following, the simulated radiation terms, heat fluxes and temperatures are discussed and compared with observations. Downward fluxes are defined to be positive. Finally, the model results are compared with the results of earlier climatological studies.

The surface energy balance

The maximum simulated net radiation values (Fig. 1) were 400–450 W m^{-2} in all three experiments on 15 and 16 August. The night-time minimum net radiation values were slightly less than -50 W m^{-2} . According to estimates based on synoptic observations (Fig. 2), the maximum net radiation was about 350 W m^{-2} on the 15th and about 430 W m^{-2} on the 16th. The night-time minimum values were between -70 and -80 W m^{-2} .

The net radiation values obtained from the model simulation correlated well with the values estimated from synoptic observations. This supports the conclusion that the radiation balance components are correctly simulated by the model. The differences between the different surface type simulations were small. The largest difference is seen in the higher maximum values for the “forest” simulation. The obvious reason for the differ-

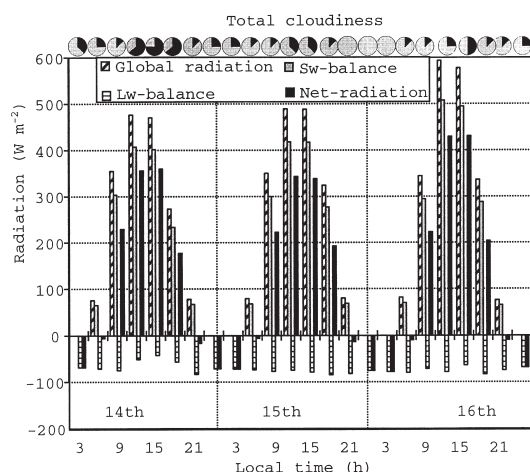


Fig. 2. Estimates of radiation balance components based on synoptic weather observations at the Kauhava weather station, 14–16 August 1997. Downward fluxes are positive.

ence is the lower albedo value used. For the first simulation night the values of the net radiation for the “wet” simulation were the highest, but on the following night the lowest. The difference was caused by cloudiness developed by the model during the first night, leading to enhanced downward long-wave radiation large enough to overcompensate the larger upward long-wave radiation connected with the higher surface temperature.

The simulated sensible and latent heat fluxes (Figs. 3 and 4) show that during the night the simulated fluxes were small and directed towards the colder surface, while during the day they were larger and directed from the surface to the overlying air. No heat flux observations were available for comparison with the simulated fluxes.

The sensible heat fluxes for the “dry” and “forest” simulations were similar to, but larger than, those for the “wet” simulations. The sensible heat flux was enhanced over the dry surface, as less energy was stored in the soil and more was used to heat or cool the air above the surface. During the night the downward latent heat flux for the “wet” simulation was smaller than for the dry simulations. This was because the dry surface was colder than the wet surface, leading to larger dew condensation on the surface, i.e., greater latent heat flux towards the surface. The daytime upward

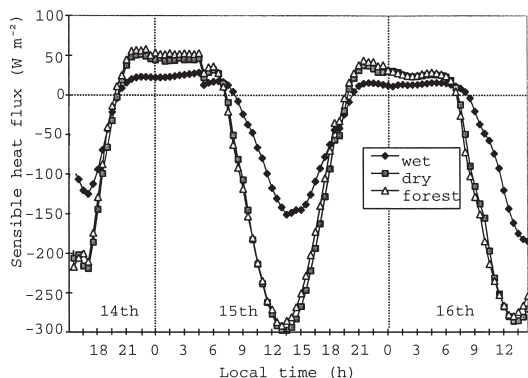


Fig. 3. Simulated sensible heat flux for the Kauhava weather station location, 14–16 August 1997. Downward fluxes are positive.

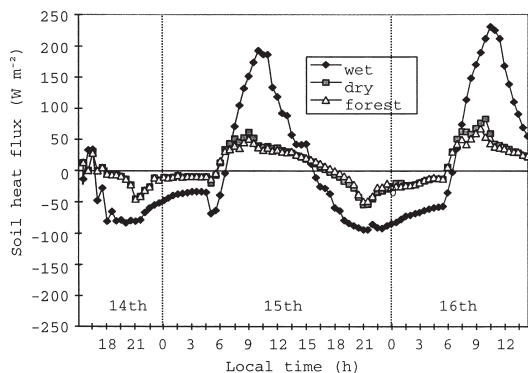


Fig. 5. Simulated net soil heat flux, as a compensation to the atmospheric forcing due to radiative, sensible and latent heat fluxes for the Kauhava weather station location, 14–16 August 1997. Downward fluxes are positive.

latent heat flux was greatest in the “wet” simulation, because evaporation from the wet surface was larger than from the dry surface. The latent heat flux above the “forest” surface was higher than above the “dry” surface, because mixing was enhanced due to the increased roughness of the forest.

In the case of the net soil heat flux, estimated by the sum of the atmospheric fluxes, the difference between the “dry” and “forest” simulations was very small and in both cases the downward daytime flux was about 50 W m^{-2} (Fig. 5). During the night the magnitude of the vertical flux was -30 W m^{-2} . In the case of the “wet” simulation, the downward flux reached values as high as 200 W m^{-2} during the day and the vertical flux during the night was about -100 W m^{-2} .

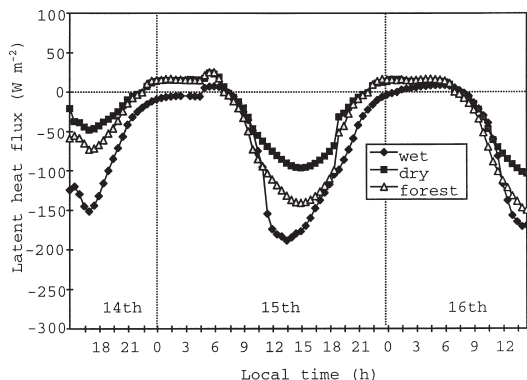


Fig. 4. Simulated latent heat flux for the Kauhava weather station location, 14–16 August 1997. Downward fluxes are positive.

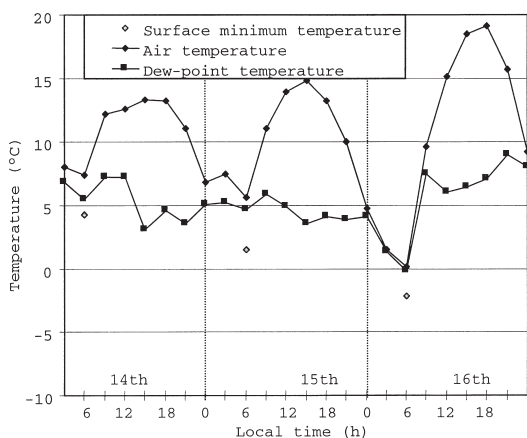


Fig. 6. Measured air temperature and dew-point temperature at a height of two metres, and surface minimum temperature at the Kauhava weather station, 14–16 August 1997.

Minimum and maximum temperatures

The observed minimum two-metre air temperatures at Kauhava (Fig. 6) were about 6°C on the 15 August and about 0°C on the 16 August. The surface minimum temperatures were a few degrees lower, i.e., about 2°C and -2°C , respectively. The lowest temperature values were found at around 5 o'clock on the 16 August. The measured daily maximum temperatures were 15°C on the 15th and 19°C on the 16th August.

In the case of the “dry” simulation, the minimum surface temperature, (T_s), on the 16 August was -6.2°C (Fig. 7) and the minimum air temperature, (T_{2m}), -5.1°C (Fig. 8). In the “forest”

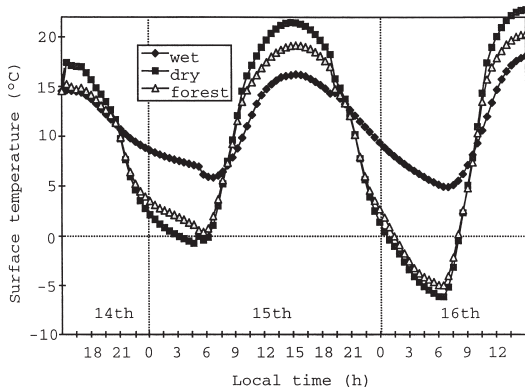


Fig. 7. Simulated surface temperature for the Kauhava weather station location, 14–16 August 1997.

simulation the corresponding values were -5.1°C and -4.4°C , and in the “wet” case 4.9°C and 5.6°C . There was thus a difference of about 10°C between the screen level temperatures of the “dry” and “wet” simulations during the second night. On the 15 August, the difference was about 7°C . The compensating effect on the minimum temperatures due the decreased surface emissivity was found to be insignificant.

The night minima were lower for dry soil but the daytime maxima were higher. The simulated maximum air temperatures (Fig. 8) varied between 15 and 20°C and the maximum surface temperatures (Fig. 7) between 16 and 22°C . The differences between the “dry” and the “wet” daytime maxima were approximately 3°C for the air and 5°C for the surface temperatures. The difference was connected with the increased sensible heat flux from the dry surface to the air compensating the decreased heat flux to the soil. The air temperatures were approximately equal in the “dry” and “forest” simulations, but the maximum surface temperature was the highest in the “dry” simulation. This can be explained by the larger upward latent heat flux over the “forest” surface.

An analysis of Eq. 6 shows how the changing soil volumetric heat capacity $\rho_s c_s$ and conductivity λ_s influenced the temperature of the uppermost soil layer T_s . In Eq. 6 the first right-hand side term describes the influence of the atmospheric forcing and the second right-hand side term the heat transfer from the uppermost to the middle layer. In the case studied, the sum of the atmospheric forcing, F , was large due to radiation, thus the first term dominates. If F is assumed to be inde-

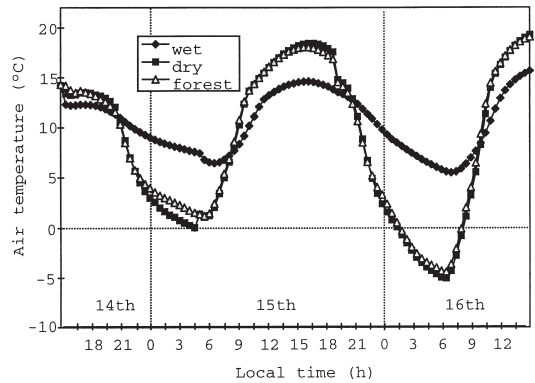


Fig. 8. Simulated air temperature for the Kauhava weather station location, 14–16 August 1997.

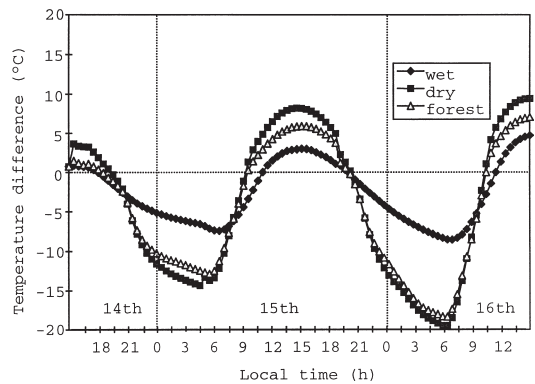


Fig. 9. Simulated temperature difference $T_s - T_d$ between the surface and middle soil layers of the model for the Kauhava weather station location, 14–16 August 1997.

pendent of T_s , then the influence of the atmospheric forcing on the temperature of the uppermost soil layer is smaller the greater the denominator $\rho_s c_s$ is (“wet” simulation). As the conductivity coefficient λ_s is greater for the “wet” case, the relative importance of the heat transfer to/from the deeper soil layers is greater than in the “dry” and “forest” cases. We should thus expect a smaller diurnal variation and lower extreme values for the surface temperature T_s in the “wet” simulation, as can be seen in Fig. 7.

An analysis of the difference $T_s - T_d$ between the surface and the middle soil layer temperatures (Fig. 9) in conditions of varying surface temperature showed that this difference is directly connected with the effectiveness of the heat conduction in the soil: the smaller the difference, the more interaction between the surface and deeper soil

temperatures there is. For the “wet” simulation, the diurnal cycle of this difference was about 7 °C, but in the “dry” and “forest” simulation cases it was as high as 30 °C.

Comparison of model simulation results with results from climatological studies

To estimate the reliability of predicted temperature changes, the results of the one-dimensional model experiments were compared with those of previous climatological studies. The model experiments were meant to give an order-of-magnitude estimate of the possible effects of the changes of soil and surface properties. They represent a typical weather situation in which maximum effects are expected to be revealed, but are of course not climatologically representative. Thus the comparison can only provide some guidance for the interpretation of results.

According to Pessi (1957), the drainage of peatlands lowers frost night minimum temperatures at the vegetation level by about 0.4–0.5 °C in June–July and 0.1–0.2 °C in May and August. Latja and Kurimo (1988), comparing two different bog areas, found that in May–September the drainage lowers surface temperatures on average by 1.1 °C and temperatures at a height of 5 cm by 0.8 °C.

In Solantie (1994), the influence of peatland draining on climate was estimated by comparing the long-term temperature time-series at the observing stations of Alajärvi (63°05'N, 24°16'E), Kauhava (63°06'N, 23°02'E) and Haapavesi (64°09'N, 25°26'E). Alajärvi is a very heavily-drained region, 56% of the nearby surroundings of the station being drained between 1951 and 1977. The most intensive draining measures were taken in the 1950s and 1970s. Kauhava and Haapavesi have smaller drainage fractions in their surroundings. All three sites were permanent and without any changes in their vicinity except for the draining during the studied period 1959–1990.

According to Solantie (1994), a drainage of 1% of the total land area lowers night minima in May–September by about 0.038 °C. The proportion of freshly-drained peatlands in the middle boreal zone of Finland reached a maximum value of 18% in the late 1970s. At that time the mean

night cooling in the zone amounted to 0.7 °C; in some regions with more extensive draining the cooling even reached 1.4 °C. This can be compared with an estimate based on the simulated temperature changes. In the simulation for the 16 August, the difference in minimum temperatures between the “wet” and “dry” simulations was about 10 °C. The mean cooling effect would therefore be 1.8 °C, assuming that the total influence of drained areas can be obtained simply by weighting the area-averaged temperature by the areal coverage of drained area (18%). For the 15 August, when the temperature difference was 7 °C, the cooling would be about 1.3 °C.

In the middle boreal zone of Finland, the albedo of peatlands is on average 14.5% and the albedo of forest 11.5% (Solantie 1988). Such a change in albedo leads to an increase in daily maximum temperatures of about 0.13 °C (Solantie 1994). In the model simulations, the change of the albedo of the dry open peatland from 14.5% to 11.5% changed the maximum local surface temperatures by about 0.4 °C, which would mean less than 0.1 °C in areal mean values.

The mean increase of the latent heat flux from conditions of drained open peatland to conditions of fully-grown forest is estimated to be about 3.5 W m⁻² (Solantie and Ekholm 1988), leading to a decrease in maximum temperatures of about 0.25 °C. The simulated difference of maximum temperatures between “dry” and “forest” experiments (with both the albedo and roughness effects included) was about 2 °C, leading to approximately the same areal mean values as estimated from observations.

Discussion

Applicability of the model simulations

The HIRLAM model was developed for limited area short-range numerical weather prediction. It includes parameterizations of the main physical processes and interactions from within the soil to upper levels of the atmosphere. The parameterized soil processes, radiation, atmospheric boundary layer, clouds and condensation interact to provide a full description of the state of the atmosphere. The one-dimensional research version of the

model also relies on the results of the full three-dimensional model run, which provides the large-scale forcing. This forcing, mainly due to development of the free atmosphere synoptic scale weather systems, is expected to give a realistic background for local sensitivity studies.

Interactions of soil-atmosphere hydrological processes, including changes in soil moisture, runoff, evaporation and condensation in the near-surface layer of the atmosphere, as well as the formation of clouds and precipitation in the atmospheric boundary layer and in the free atmosphere, are complicated and computationally demanding. Changes in model cloudiness lead to changes of predicted temperatures through radiation parameterization. In the present study, the effect of soil moisture changes on temperature was estimated independently of the hydrological cycle of the model by introducing the soil properties for dry and saturated peatland into the equations of soil thermal diffusion.

The values of soil moisture were far from saturation even in the case of "wet" simulation. However, as in the present HIRLAM model there is no direct functional dependence between the soil moisture and the soil thermal properties, the results are not influenced by this omission. A scheme including such dependence, based on Noilhan and Planton (1989), will be included in a new HIRLAM version presently under development.

Two of the proposed processes connected with the later phases of peatland draining, namely the increased evapotranspiration and the formation of a canopy shelter by the fully-grown forest, could not be fully described by the model simulations because of the simplified parameterization of the vegetation cover. In the model the "forest" is defined by the short-wave albedo, long-wave emissivity and roughness length of the surface. The model forest does not have any vertical structure nor are any biological processes included.

One-dimensional simulations are able to show the possible maximum local influence of draining on the near-surface temperatures. Estimation of the regional impact based only on the areal coverage of drained areas is a simplification. Obviously, the influence is different depending upon whether the drained areas are in small patches, or they comprise a single large entity. Realistic results taking into account all atmos-

phere-soil interactions over large drained areas could be obtained only through full three-dimensional climate simulations over a longer time-period, such as a whole summer.

The long-term regional consequences of draining

On the basis of climate statistics, it is possible to relate the temperature minima to the duration of the frost-free period, i.e., the period between the latest date in spring and the earliest in autumn with screen temperatures below 0 °C. In the middle boreal zone the frost-free period is short and comprises only the warmest time of the year. Consequently, even slight changes in the mean level of minima are significant for the length of this period. Solantie (1998) estimated that during the period 1963–1982 the mean shortening of the duration of the frost-free period in the middle boreal zone due to draining is 14 days, in some regions even as much as 34 days.

In winter the incoming solar radiation is insignificantly small and the ground is snow-covered. The drainage only influences the long-wave radiation balance. The shelter effect due to the growing forest canopy becomes effective about 15 years after drainage. Afforestation of 1% of the land area raises the average daily temperature minima in November–May by about 0.03 °C (Solantie 1994 and Solantie 1998). The present mean proportion of afforested area in the middle boreal zone in Finland, excluding the areas where draining has failed, is about 18%. The rise in the daily winter-time minima corresponding to this areal coverage amounts to 0.5 °C. The effect of afforestation on annual minima is about twice as great. In some regions, where afforested peatlands comprise 45% of the area, the increased shelter has raised annual minima up to 1997 by 4 °C, of which 3.4 °C occurred during the period 1966–1990 (Solantie 1998). This positive effect, in fact an additional greenhouse effect, will be permanent. It obviously has ecological consequences by influencing the wintering conditions of vegetation and insect fauna.

After afforestation, daily minima in summer have risen close to their levels before drainage. The net loss of energy from the surface through

long-wave infrared radiation has decreased due to the formation of the canopy. On the other hand, on many barren bogs afforestation has failed, and no canopy has ever formed. The fraction of peatlands where draining and afforestation has failed is about 20% of the total drained peatland area (Solantie 1998). Thus, particularly during dry and hot summers like 1997, a significant cooling effect from the drainage can still be noticed.

Conclusions

Massive draining of peatlands over a period of a quarter of century, mainly in 1960–1980, has been in some parts of Finland the most extensive man-made manipulation of the soil-vegetation system ever performed in this country. The drained area comprised twice the area cleared for cultivation during the last two thousand years.

Numerical case study simulations support the conclusion of earlier climatological studies on the transient cooling effect of the drainage. The change of soil heat conductivity connected with the draining leads to a decrease of heat flux to and from the soil. In clear and calm late summer conditions, when the nights are relatively long and the upward net long-wave radiation cools the surface effectively, the change in the local minimum temperature was found to be up to ten degrees, when simulated conditions for wet and dry peatland were compared.

Changes in the surface properties — the short-wave albedo, long-wave emissivity and surface roughness — were found to have only a minor influence on near-surface temperatures both shortly after the drainage and later, when the forests become fully grown. This conclusion is also in accordance with the former empirical results.

References

- Bird R. & Hulstrom, R. L. 1981. Direct insolation models. *Trans. ASME Journal of Solar Energy Engineering* 103: 182–192.
- Bonan G.B., Pollard D. & Thompson S.L. 1992. Effects of boreal forest vegetation on global climate. *Nature* 359: 716–718.
- Brutsaert W. 1982. *Evaporation into the atmosphere*, D. Reidel Publishing Company, Dordrecht, 299 pp.
- Finnish Forest Research Institute 1992. *Yearbook of forest statistics* 1990–91, 281 pp.
- Heikinheimo M. & Fougstedt B. 1992. Statistics of soil temperature in Finland 1971–1990. *Meteorological publications* 22. Finnish Meteorological Institute, Helsinki, 75 pp.
- Iqbal M. 1983. *An Introduction to solar radiation*. Ontario: Academic press Canada, 390 pp.
- Källen E. (ed.) 1996. *HIRLAM documentation manual. System 2.5. June 1996*. Available from SMHI, S-60176, Norrköping, Sweden.
- Latja A. & Kurimo H. 1988. Temperature changes in the soil and close to the ground on wetlands drained for forestry. Symposium on the hydrology of wetlands in temperate and cold regions. *The publications of the Academy of Finland* 4/1988. 46–51.
- Louis J.F. 1979. A parametric model of vertical eddy fluxes in the atmosphere. *Boundary Layer Meteorol.* 17: 187–202.
- Manabe S. & Strickler R.F. 1964. Thermal equilibrium of an atmosphere with convective adjustment. *J. Atmos. Sci.* 21: 433–444.
- Noilhan J. & Planton S. 1989. A simplified parameterization of land surface. *Mon. Wea. Rev.* 117: 536–549.
- Oke T. 1987. *Boundary layer climates*. Routledge, London, 435 pp.
- Pessi Y. 1957. Suon ojituksen ja viljelykseenoton vaikutukset maan ja maanpinnan läheisen ilman lämpöoloihin. *Suo* 4/1957: 37–41.
- Savijärvi H. 1990. Fast radiation parameterization schemes for mesoscale and short-range forecast models. *J. Appl. Meteor.* 29: 437–447.
- Savijärvi H. 1992. On surface temperature and moisture prediction in atmospheric models. *Beitr. Phys. Atmosph.* 65: 281–292.
- Sellers W.D. 1965. *Physical climatology*. The University of Chicago press, 272 pp.
- Shukla J., Nobre C.A. & Sellers P.J. 1990. Amazon deforestation and climate change. *Science* 247: 1322–1325.
- Solantie R. & Ekholm E. 1984. Water balance in Finland during the period 1961–1975 as compared to 1931–1960. *Publications of the Water Research Institute* 59, National Board of Waters in Finland, 53 pp.
- Solantie R. 1988. Albedo in Finland on the basis of observations on aircraft. *Meteorological publications* 12. Finnish Meteorological Institute, Helsinki, 106 pp.
- Solantie R. 1994. Suurten suo-ojitusten vaikutus ilman lämpötilaan erityisesti Alajärven Möksyn havaintojen perusteella. *Meteorological publications* 29. Finnish Meteorological Institute, Helsinki, 40 pp. [In Finnish with English summary]
- Solantie R. 1998. Suurten suo-ojitusten vaikutus pakkas-ettoman ajan pituuteen ja lämpötilan vuosiminimiin 1961–1990 sekä lämpötilatrendeihin vuodesta 1990. *Meteorological publications* 38. Finnish Meteorological Institute, Helsinki, 43 pp. [In Finnish with English summary]
- Sundqvist H., Berge E. & Kristjansson J.E. 1989. Conden-

sation and cloud parameterization studies with a mesoscale numerical weather prediction model. *Mon. Wea. Rev.* 117: 1641–1656.

Sundqvist H. 1993. Inclusion of ice phase hydrometeors in cloud parameterization for mesoscale and largescale models. *Beitr. Phys. Atmosph.* 66: 137–147.

Venäläinen A. & Nordlund A. 1988. Kasvukauden ilmastotiedotteen sisältö ja käyttö, *Raportteja* No. 1988:6, Ilmatieteen laitos, Helsinki, 63 pp.

Venäläinen A & Heikinheimo M. 1997. The spatial variation of long-term mean global radiation in Finland. *Int. J. Climatol.* 17: 415–426.

Appendix

Description of parameterizations used for calculation of global radiation and long-wave radiation balance based on synoptic weather observations.

In this parameterization global solar radiation is calculated as the sum of direct and diffuse radiation. The direct solar radiation is calculated using a formula by Bird and Hulstrom (1981)

$$R_{\text{dir}} = 0.9751 R_o (\sin \gamma) \tau_R \tau_g \tau_w \tau_a \tau_o \quad (\text{A1})$$

where R_{dir} is the direct radiation on a horizontal surface, R_o is the solar flux on a surface exposed normal to the sun's rays in the absence of the atmosphere, γ is the sun's elevation angle, τ_R is the broadband transmittance by Rayleigh scattering, τ_g is the transmittance by uniformly mixed gases, τ_w is the transmittance by water vapour, τ_a is the transmittance by aerosols and τ_o is the transmittance by ozone. The factor 0.9751 is included because the spectral interval considered is 0.3–3.0 μm . The formulae for the calculation of the parameters needed in Eq. A1 were taken from Iqbal (1983).

The diffuse radiation R_{dif} was calculated as the sum of three terms (Iqbal 1983)

$$R_{\text{dif}} = R_{\text{difr}} + R_{\text{difa}} + R_{\text{difm}}, \quad (\text{A2})$$

where R_{difr} is the Rayleigh-scattered and R_{difa} is the aerosol-scattered diffuse radiation after the first pass through the atmosphere, and R_{difm} is the multiply-reflected radiation. Multiply-reflected radiation is the component of global radiation reflected from the earth's surface to the atmosphere and from the atmosphere back to earth.

The global solar radiation under a cloudy sky can be estimated by adding one more transmittance factor, the transmittance by clouds τ_c . Thus the equation for global radiation under a cloudy sky is

$$R_{\text{gc}} = \tau_c R_{\text{go}}, \quad (\text{A3})$$

where R_{go} is the global radiation under a cloudless sky. According to Manabe (1964) the transmittance function for multiple layers of clouds is

$$\tau_c = \prod_{i=1}^{n_c} [1 - c_i (1 - \psi_i)], \quad (\text{A4})$$

where c_i is the amount and ψ_i the transmittance of each individual cloud layer.

The amount and type of each individual cloud layer is not available from a standard synoptic weather observation; the synoptic cloud codes were transformed into the format needed in the parameterization based on a formulation described in Venäläinen and Nordlund (1988).

Global radiation was calculated as the sum of direct, Rayleigh-scattered diffuse, aerosol-scattered diffuse and multiply reflected diffuse radiation. Multiply reflected radiation mainly results from the cloud layer in the case of cloudy conditions and thus Eq. A3 was modified to

$$R_{\text{gc}} = (R_{\text{dir}} + R_{\text{difr}} + R_{\text{difa}}) \tau_c + R_{\text{difm}}, \quad (\text{A5})$$

The atmospheric albedo is needed to calculate R_{difm} and in the case of cloudy conditions this was taken as the sum of the clear-sky atmospheric albedo and the cloud transmittance, τ_c (Eq. A4). The surface albedo used in the calculations was 14.5%.

The formula used to estimate the net long-wave radiation under a clear sky (RL_{nc}) is taken from Brutsaert (1982).

$$RL_{\text{nc}} = \varepsilon \sigma T (1.28 (e/T)^{1/7} - 1), \quad (\text{A6})$$

where ε is the surface emissivity, σ is the Stefan-Boltzman constant and e and T are the water vapour pressure (hPa) and air temperature (Kelvins), respectively, at a height of 2 metres. A constant value (0.98) was used for the surface emissivity. The influence of clouds on the long-wave radia-

tion balance was estimated using a widely-used formula that can be found in, e.g., Sellers (1965) (Eq. A7).

$$Rl = RL_{nc}(1 - kn^2), \quad (A7)$$

where k is an empirical constant whose value depends on cloud type, and n is the total cloudiness. After Sellers (1965) k is 0.85 in the case of low and medium clouds and 0.25 for high clouds.

Received 1 June 1998, accepted 15 December 1998